# CROSS-LAYER COMBINING OF QUEUING WITH ADAPTIVE MODULATION AND CODING OVER WIRELESS LINKS

Qingwen Liu[1], Shengli Zhou[2], and Georgios B. Giannakis[1]
[1]Dept. of ECE, Univ. of Minnesota, Minneapolis, MN
[2]Dept. of ECE, Univ. of Connecticut, Storrs, CT

## ABSTRACT

*Assuming there are always sufficient data waiting to be transmitted, adaptive modulation and coding (AMC) at the physical layer have been traditionally designed separately from higher layers. However, this assumption is not always valid when queuing effects are taken into account at the data link layer. In this paper, we analyze the performance of a wireless system with finite-length queuing and AMC. We characterize the queuing service process induced by AMC, and derive the recursion of the queue state. We then construct a finite state Markov chain (FSMC) with a state pair containing both the queue and the queue server state, and compute its stationary distribution. The latter enables us to derive closed-form expressions for the packet loss rate and the average throughput. Guided by our performance analysis, we also introduce a cross-layer design, which optimizes the target packet error rate in AMC at the physical layer, to minimize the packet loss rate and maximize the average throughput, when combined with a finite-length queue at the data link layer.*

## I. INTRODUCTION

To enhance the spectral efficiency while adhering to a target error performance over wireless channels, adaptive modulation and coding (AMC) have been widely used to match transmission parameters to time-varying channel conditions; see e.g., [1] and references therein.

However, existing AMC schemes rely on the salient assumption that data are continuously available at the transmitter: whatever modulation-coding modes are chosen at the physical layer to match the wireless channel, there are sufficient data waiting to be transmitted in the queues (buffers) at the data link layer. However, in practical communication systems with randomly arriving data streams, the queues may be empty from time to time, even though the wireless channel can accommodate transmissions. This leads to a dynamic behavior of the queue, the impact of which on AMC has not been investigated so far.

On the other hand, the service process of the queue feeding an AMC module, is no longer deterministic, which is not the case with non-adaptive modulations. Indeed, the service process is affected by the wireless medium, and depends on how the AMC module adapts its parameters to channel variations. Furthermore, the queue length (buffer size) is finite in practice. When the buffer is full and overflow occurs, excess packets have to be dropped. The effect of overflow also needs to be taken into account when analyzing the overall system performance.

Prepared through collaborative participation in the Communications and Networks Consortium sponsored by the U. S. Army Research Laboratory under the Collaborative Technology Alliance Program, Cooperative Agreement DAAD19-01-2-0011. The U. S. Government is authorized to reproduce and distribute reprints for Government purposes notwithstanding any copyright notation thereon.

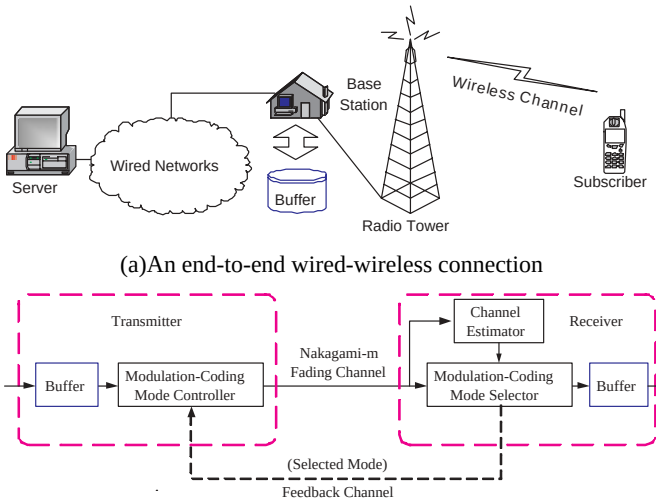


(a)An end-to-end wired-wireless connection

(b)The wireless link with combined queuing and AMC

Fig. 1. The overall system diagram

The interaction of queuing with AMC provides interesting design problems. Consider for instance the packet loss rate of the end-to-end system, that is defined as the ratio of the number of incorrectly received packets at the destination over those transmitted from the source. The packet loss rate is affected by both the queuing overflow, and the packet reception error.

In this paper, we analyze jointly finite-length queuing and AMC. We first characterize the queuing service process dictated by AMC, and derive the queue state recursion. Then, we construct a finite state Markov chain (FSMC) with a state pair containing both the queue and the queue server state, and compute its stationary distribution. The latter enables us to obtain the packet loss rate and the average throughput, in closed-form. Based on the performance analysis, we develop a cross-layer design, which optimizes the target packet error rate of AMC at the physical layer, to minimize the system packet loss rate and maximize the average throughput, when combined with a finite-length queue at the data link layer.

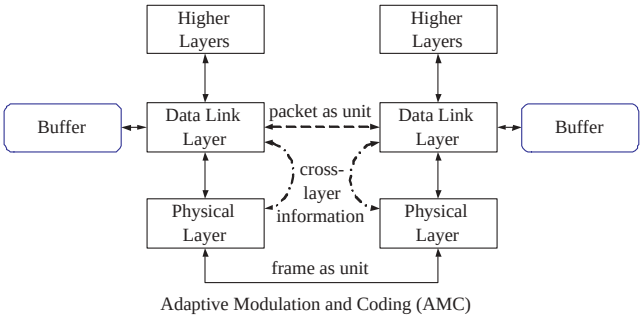


Fig. 2. The cross-layer structure combining AMC with queuing

## II. MODELING

### A. System and Channel Models

Fig. 1(a) illustrates an end-to-end connection between a server (source) and a subscriber (destination), which includes a wireless link with a single-transmit and a single-receive antenna. We focus on the downlink here, although our results are applicable to the uplink as well. As depicted in Fig. 1(b), a finite-length queue (buffer) is implemented at the transmitter, and operates in a first-in-first-out (FIFO) mode. The queue feeds the AMC controller at the transmitter. The AMC selector is implemented at the receiver. The layer structure of the proposed system is shown in Fig. 2. The processing unit at the data link layer is a packet, which comprises multiple information bits. On the other hand, the processing unit at the physical layer is a frame, which consists of multiple transmitted symbols. The packet and frame structures will be detailed soon.

We assume that multiple transmission modes are available, with each mode representing a pair of a specific modulation format, and a forward error correcting (FEC) code, as in the HIPERLAN/2, and the IEEE 802.11a standards. Based on channel state information (CSI) estimated at the receiver, the AMC selector determines the modulation coding pair (mode), which is sent back to the transmitter via a feedback channel, for the AMC controller to update the transmission mode. Coherent demodulation and maximum-likelihood (ML) decoding are employed at the receiver. The decoded bit streams are mapped to packets, which are pushed upwards to layers above the physical layer.

We consider the following group of transmission modes:
**TM**: Convolutionally coded $M_n$-ary rectangular or square QAM modes, adopted from the HIPERLAN/2 and IEEE 802.11a standards [3], which are listed under Table I, in a rate ascending order.
Although we will focus on TM in this paper, other transmission modes can be similarly constructed.

At the *physical layer*, we deal with frame by frame transmissions, where each frame contains a fixed number of symbols ($N_s$). Given a fixed symbol rate as in [3], the frame duration ($T_f$ seconds) is constant, and represents the time-unit throughout this paper. Each frame at the physical layer may contain one or more packets from the data link layer. The packet and frame structures are depicted in Fig. 3. Each packet contains a fixed number of bits ($N_b$), which include packet header, payload, and cyclic redundancy check (CRC) bits. After modulation and coding with mode $n$ of rate $R_n$ (bits/symbol), each packet is mapped to a symbol-block containing $N_b/R_n$ symbols. Multiple such blocks, together with $N_c$ pilot symbols and control parts, constitute one frame to be transmitted at the physical layer, as in the HIPERLAN/2, and the IEEE 802.11a standards [3]. If mode $n$ is used, it follows that the number of symbols per frame is $N_s = N_c + N_p N_b/R_n$, which implies that $N_p$ (the number of packets per frame) depends on the chosen mode.

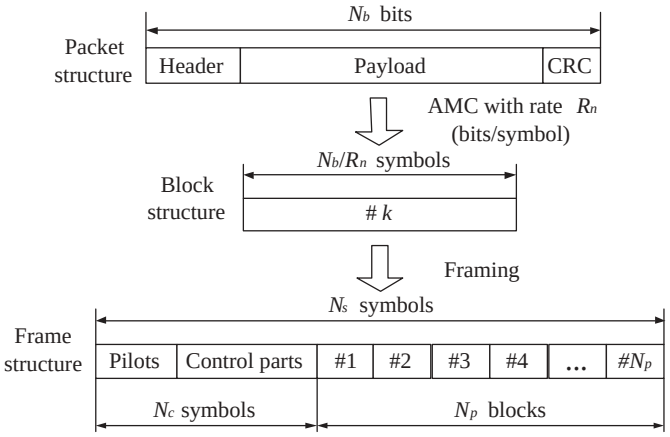


Fig. 3. The packet and frame structures

At the *data link layer*, the queue has finite-length (capacity) of $K$ packets. For analytical convenience, the arrival process upon the queue is modeled as Poisson distributed with rate $\lambda T_f$ packets/time-unit, as in [2].

We next list the assumptions adopted in this paper:
**A1**: The channel is frequency flat, and remains invariant per frame, but is allowed to vary from frame to frame. This corresponds to a block fading channel model, which is suitable for slowly-varying fading channels. As a consequence, AMC is adjusted on a frame-by-frame basis [4].
**A2**: Perfect channel state information (CSI) is available at the receiver using training-based channel estimation. The corresponding mode selection is fed back to the transmitter without error and latency, as in [1].
**A3**: When the queue is full, arriving packets are dropped and are not recovered by end-to-end (server-to-subscriber) or link-layer retransmissions, as in video transmissions via UDP (user datagram protocol) [10].
**A4**: Error detection based on CRC is perfect, and the serial number as well as CRC parity bits in each packet are not included in the throughput calculation.
**A5**: If a packet is received incorrectly at the receiver after error detection, we drop it, and declare packet loss [10].

For flat fading channels adhering to A1, the channel quality can be captured by a single parameter, namely the

TABLE I

TRANSMISSION MODES IN TM WITH CONVOLUTIONALLY CODED MODULATION

| | Mode 1 | Mode 2 | Mode 3 | Mode 4 | Mode 5 |
|---|---|---|---|---|---|
| Modulation | BPSK | QPSK | QPSK | 16-QAM | 64-QAM |
| Coding rate $R_c$ | 1/2 | 1/2 | 3/4 | 3/4 | 3/4 |
| $R_n$ (bits/sym.) | 0.50 | 1.00 | 1.50 | 3.00 | 4.50 |
| $a_n$ | 274.7229 | 90.2514 | 67.6181 | 53.3987 | 35.3508 |
| $g_n$ | 7.9932 | 3.4998 | 1.6883 | 0.3756 | 0.0900 |
| $\gamma_{pn}$(dB) | -1.5331 | 1.0942 | 3.9722 | 10.2488 | 15.9784 |

(The generator polynomial of the mother code is $g = [133, 171]$. )

received signal-to-noise ratio (SNR) $\gamma$. Since the channel varies from frame to frame, we adopt the general Nakagami-$m$ model to describe $\gamma$ statistically [7]. The received SNR $\gamma$ per frame is thus a random variable with a Gamma probability density function (pdf):

$$p_\gamma(\gamma) = \frac{m^m \gamma^{m-1}}{\bar{\gamma}^m \Gamma(m)} \exp\left(-\frac{m\gamma}{\bar{\gamma}}\right), \qquad (1)$$

where $\bar{\gamma} := E\{\gamma\}$ is the average received SNR, $\Gamma(m) := \int_0^\infty t^{m-1}\exp(-t)dt$ is the Gamma function, and $m$ is the Nakagami fading parameter ($m \geq 1/2$). We choose the Nakagami-$m$ channel model because it encompasses a large class of fading channels; e.g., it includes the Rayleigh channel as a special case when $m = 1$ [7].

### *B. Adaptive Modulation and Coding*

The objective of AMC is to maximize the data rate by adjusting transmission parameters to the available CSI, while maintaining a prescribed packet error rate $P_0$. Let $N$ denote the total number of transmission modes available ($N = 5$ for TM). As in [1], we assume constant power transmission, and partition the entire SNR range into $N + 1$ non-overlapping consecutive intervals, with boundary points denoted as $\{\gamma_n\}_{n=0}^{N+1}$. In this case,

$$\text{mode } n \text{ is chosen, when } \gamma \in [\gamma_n, \gamma_{n+1}). \qquad (2)$$

To avoid deep channel fades, no data are sent when $\gamma_0 \leq \gamma < \gamma_1$, which corresponds to the mode $n = 0$ with rate $R_0 = 0$ bits/symbol. The design objective for AMC is to determine the boundary points $\{\gamma_n\}_{n=0}^{N+1}$.

For simplicity, we approximate the packet error rate (PER) in the presence of additive white Gaussian noise (AWGN), as [4, eq. (5)]:

$$\text{PER}_n(\gamma) \approx \begin{cases} 1, & \text{if } 0 < \gamma < \gamma_{pn}\,, \\ a_n \exp\left(-g_n\gamma\right), & \text{if } \gamma \geq \gamma_{pn}\,, \end{cases} \qquad (3)$$

where $n$ is the mode index, $\gamma$ is the received SNR, and the mode-dependent parameters $a_n$, $g_n$, and $\gamma_{pn}$ are obtained by fitting (3) to the exact PER. With packet length $N_b = 1,080$, the fitting parameters for transmission modes TM are provided in Table I [4]. Based on (1) and (2), the mode $n$ will be chosen with probability [1, eq. (34)]:

$$\Pr(n) = \int_{\gamma_n}^{\gamma_{n+1}} p_\gamma(\gamma)d\gamma = \frac{\Gamma(m, \frac{m\gamma_n}{\bar{\gamma}}) - \Gamma(m, \frac{m\gamma_{n+1}}{\bar{\gamma}})}{\Gamma(m)},$$

where $\Gamma(m, x) := \int_x^\infty t^{m-1}\exp(-t)dt$ is the complementary incomplete Gamma function. Let $\overline{\text{PER}}_n$ be the average PER corresponding to mode $n$. In practice, we have $\gamma_n > \gamma_{pn}$, and thus obtain $\overline{\text{PER}}_n$ as (c.f. [1, eq.(37)]):

$$\begin{aligned}\overline{\text{PER}}_n &= \frac{1}{\Pr(n)} \int_{\gamma_n}^{\gamma_{n+1}} a_n \exp(-g_n\gamma) p_\gamma(\gamma)d\gamma \\ &= \frac{a_n m^m}{\Pr(n)\Gamma(m)\bar{\gamma}^m} \frac{\Gamma(m, b_n\gamma_n) - \Gamma(m, b_n\gamma_{n+1})}{(b_n)^m},\end{aligned}$$

where $b_n := m/\bar{\gamma} + g_n$, $n = 1, \ldots, N$. The average PER of AMC is computed as the ratio of the average number of packets in error over the total average number of transmitted packets [1]:

$$\overline{\text{PER}} = \frac{\sum_{n=1}^N R_n \Pr(n) \overline{\text{PER}}_n}{\sum_{n=1}^N R_n \Pr(n)}. \qquad (4)$$

We want to find the thresholds $\{\gamma_n\}_{n=0}^{N+1}$, so that the prescribed $P_0$ is achieved for each mode: $\overline{\text{PER}}_n = P_0$, which naturally leads to $\overline{\text{PER}} = P_0$ based on (4). Given $P_0$, $\bar{\gamma}$, and $m$, the following threshold searching algorithm determines $\{\gamma_n\}_{n=0}^{N+1}$, and guarantees that $\overline{\text{PER}}_n$ is exactly $P_0$:

**Step 1**: Set $n = N$, and $\gamma_{N+1} = +\infty$.

**Step 2**: For each $n$, search for the unique $\gamma_n \in [0, \gamma_{n+1}]$ that satisfies: $\overline{\text{PER}}_n = P_0$ .

**Step 3**: If $n > 1$, set $n = n - 1$, and go to Step 2; otherwise, go to Step 4.

**Step 4**: Set $\gamma_0 = 0$.

The SNR region $[\gamma_n, \gamma_{n+1})$ corresponding to transmission mode $n$ constitutes the channel state indexed by $n$. To describe the transition of these channel states, we rely on a FSMC model, which we develop next.

### *C. Finite State Markov Chain Channel Model*

Assuming slow fading conditions so that transition happens only between adjacent states, the probability of tran-

sition exceeding two consecutive states is zero [9]; i.e.,

$$P_{l,n} = 0, \quad |l-n| \geq 2\,. \tag{5}$$

The adjacent-state transition probability can be determined by [9, eq. (10) and (11)]:

$$P_{n,n+1} = \frac{N_{n+1}T_f}{\Pr(n)}, \quad P_{n,n-1} = \frac{N_n T_f}{\Pr(n)}, \tag{6}$$

where $N_n$ is the cross-rate of mode $n$ (either upward or downward). $N_n$ can be estimated as [8, eq. (17)]:

$$N_n = \frac{\sqrt{2\pi} f_d}{\Gamma(m)} \left(\frac{m\gamma_n}{\bar{\gamma}}\right)^{m-\frac{1}{2}} \exp\left(-\frac{m\gamma_n}{\bar{\gamma}}\right), \tag{7}$$

where $f_d$ denotes the mobility-induced Doppler spread. The probability of staying at the same state $n$ is:

$$P_{n,n} = \begin{cases} 1 - P_{n,n+1} - P_{n,n-1}, & \text{if } 0 < n < N, \\ 1 - P_{0,1}, & \text{if } n = 0, \\ 1 - P_{N,N-1}, & \text{if } n = N. \end{cases} \tag{8}$$

In summary, we model the channel as a FSMC with an $(N+1)\times(N+1)$ state transition matrix:

$$\mathbf{P}_c = \begin{bmatrix} P_{0,0} & P_{0,1} & 0 & \cdots & 0 \\ P_{1,0} & P_{1,1} & P_{1,2} & \cdots & 0 \\ \vdots & \ddots & \ddots & \ddots & \vdots \\ 0 & \cdots & P_{N-1,N-2} & P_{N-1,N-1} & P_{N-1,N} \\ 0 & \cdots & 0 & P_{N,N-1} & P_{N,N} \end{bmatrix}. \tag{9}$$

## III. Finite-Length Queuing with AMC

We first characterize the queuing service process dictated by AMC, and specify the queue state recursion. Then, we construct an enlarged FSMC with a state pair containing both the queue and the queue server state, and compute its stationary distribution. The latter enables us to obtain the packet loss rate and the average throughput.

### A. The Queuing Service Process based on AMC

Different from non-adaptive modulations, AMC dictates a dynamic, rather than deterministic, service process for the queue, with a variable number of packets transmitted per time unit. Let $t$ index the time units, and $C_t$ (packets/time-unit) denote the number of packets transmitted using AMC at time $t$. Corresponding to each transmission mode $n$, let $c_n$ denote the number of packets transmitted per time-unit. We then have:

$$C_t \in \mathcal{C}, \qquad \mathcal{C} := \{c_0, c_1, \ldots, c_N\}\,, \tag{10}$$

where $c_n$ takes positive integer values (see also Fig. 3). Suppose for the rate $R = 1$ transmission mode (e.g., Mode 2 in TM), a total of $b$ packets are accommodated per frame. We then have $c_n = bR_n$, where $b$ is up to the designer's choice.

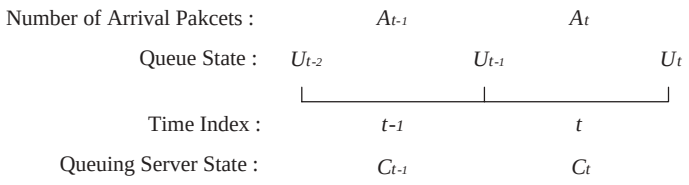


Fig. 4. The recursive queuing model

As specified by (10), the AMC module yields a queue server with a total of $N+1$ states $\{c_n\}_{n=0}^N$, with the service process $C_t$ representing the evolution of server states. Since the AMC mode $n$ is chosen when the channel enters the state $n$, we model the service process $C_t$ as a FSMC with transition matrix given by (9).

### B. Queue State Recursion

Having modeled the queuing service process, we now focus on the queue itself. Let $U_t$ denote the queue state (the number of packets in the queue) at the end of time-unit $t$, or, at the beginning of time-unit $t+1$, as shown in Fig. 4. Let $A_t$ denote the number of packets arriving at time $t$. It is clear that $U_t \in \mathcal{U} := \{0, 1, \ldots, K\}$, and $A_t \in \mathcal{A} := \{0, 1, \ldots, \infty\}$. We assume that $A_t$ is Poisson distributed with parameter $\lambda T_f$ [2, pp. 164]:

$$P(A_t = a) = \begin{cases} \frac{(\lambda T_f)^a \exp(-\lambda T_f)}{a!}, & \text{if } a \geq 0\,, \\ 0, & \text{otherwise}\,, \end{cases} \tag{11}$$

and ensemble-average $E\{A_t\} = \lambda T_f$.

We assume that the transmitter first moves packets out of the queue at the beginning of time $t$, based on the server state $C_t$. Arriving packets are placed into the queue throughout the time slot $t$. After moving $C_t$ packets out of the queue, the number of packets left in the queue is:

$$L_t = \max\{0, U_{t-1} - C_t\}. \tag{12}$$

The number of free slots in the queue at the beginning of time $t$ is thus:

$$F_t = K - L_t = K - \max\{0, U_{t-1} - C_t\}. \tag{13}$$

Let us now focus on the packets arriving at time $t$. If $A_t \leq F_t$, all arrivals enter the queue, and the queue state becomes $U_t = L_t + A_t$. On the other hand, if $A_t > F_t$, only $F_t$ packets enter the queue, and the remaining $A_t - F_t$ packets are dropped. The corresponding queue state becomes $U_t = K$. The recursion of the queue state can therefore be summarized as follows:

$$U_t = \min\{K,\ \max\{0, U_{t-1} - C_t\} + A_t\}. \tag{14}$$

To analyze the system performance, we need to find the stationary distribution of the queue state. Notice that the

recursion of queue state $U_t$ is affected by the server state $C_t$. To find the stationary distribution, we will construct an enlarged FSMC with a state pair containing both the queue and the server states, similar to the approach taken by [6].

### C. Queuing Analysis

Let $(U_{t-1}, C_t)$ denote the pair of queue and server states, and $P_{(u,c),(v,d)}$ denote the transition probability from $(U_{t-1} = u, C_t = c)$ to $(U_t = v, C_{t+1} = d)$, where $(u, c) \in \mathcal{U} \times \mathcal{C}$, and $(v, d) \in \mathcal{U} \times \mathcal{C}$. We organize the state transition probability matrix in a block form:

$$\mathbf{P} = \begin{bmatrix} \mathbf{A}_{0,0} & \cdots & \mathbf{A}_{0,K} \\ \vdots & \ddots & \vdots \\ \mathbf{A}_{K,0} & \cdots & \mathbf{A}_{K,K} \end{bmatrix}, \tag{15}$$

where the sub-matrix $\mathbf{A}_{u,v}$ is defined as:

$$\mathbf{A}_{u,v} = \begin{bmatrix} P_{(u,c_0),(v,c_0)} & \cdots & P_{(u,c_0),(v,c_N)} \\ \vdots & \ddots & \vdots \\ P_{(u,c_N),(v,c_0)} & \cdots & P_{(u,c_N),(v,c_N)} \end{bmatrix}. \tag{16}$$

We next simplify $P_{(u,c),(v,d)}$ as:

$$\begin{aligned} &P_{(u,c),(v,d)} \\ &:= P(U_t = v, C_{t+1} = d | U_{t-1} = u, C_t = c) \\ &= P(C_{t+1} = d | C_t = c) P(U_t = v | U_{t-1} = u, C_t = c) \\ &= P_{c,d} \cdot P(U_t = v | U_{t-1} = u, C_t = c) \,, \end{aligned} \tag{17}$$

where the second equality follows from the fact that $C_{t+1}$ only depends on $C_t$. As explained in Section III-A, $P(C_{t+1} = d | C_t = c)$ can be found from the entries of $\mathbf{P}_c$ in (9). Based on (14), one can easily verify that:

$$P(U_t = v | U_{t-1} = u, C_t = c) = \tag{18}$$
$$\begin{cases} P(A_t = v - \max\{0, u - c\}), & \text{if } 0 \le v < K, \\ 1 - \sum\limits_{0 \le v < K} P(U_t = v | U_{t-1} = u, C_t = c) \,, & \text{if } v = K \end{cases}$$

Combining (16), (17), and (18), we obtain $\mathbf{P}$ in (15).

In [5], we prove that the stationary distribution of the FSMC $(U_{t-1}, C_t)$ exists and is unique. Let this stationary distribution be:

$$P(U = u, C = c) := \lim_{t \to \infty} P(U_{t-1} = u, C_t = c) \,. \tag{19}$$

For notational convenience, let $\pi_{(u,c)} := P(U = u, C = c)$, and define the row vector:

$$\boldsymbol{\pi} = [\pi_{(0,c_0)}, \ldots, \pi_{(0,c_N)}, \ldots, \pi_{(K,c_0)}, \ldots, \pi_{(K,c_N)}]. \tag{20}$$

The stationary distribution of $(U_{t-1}, C_t)$ can then be computed from the equality (see also [2, pp. 259]):

$$\boldsymbol{\pi} = \boldsymbol{\pi}\mathbf{P}, \quad \sum_{u \in \mathcal{U}, c \in \mathcal{C}} \pi_{(u,c)} = 1, \tag{21}$$

which implies that $\boldsymbol{\pi}$ is the left eigenvector of $\mathbf{P}$ corresponding to the eigen-value 1.

### D. System Performance

We are now ready to evaluate the system performance with a finite-length queue and AMC. Let $P_d$ denote the packet dropping (overflow or blocking) probability upon queuing. A packet from the source is correctly received by the subscriber, only if it is not dropped from the queue (with probability $1 - P_d$), and it is correctly received through the wireless channel (with probability $1 - P_0$). Hence, the overall packet loss rate, defined as the ratio of the number of incorrectly received packets at the destination over those transmitted from the source, is:

$$\xi = 1 - (1 - P_d) \cdot (1 - P_0) \,. \tag{22}$$

The average throughput can then be evaluated as:

$$\eta = E\{A_t\}(1 - \xi) = (\lambda T_f) \cdot (1 - P_d) \cdot (1 - P_0) \,. \tag{23}$$

Hence, to evaluate the system performance in terms of packet loss rate and average throughput, we need $P_d$.

Let $D_t$ denote the number of packets dropped at time $t$. From (13), we express $D_t$ as:

$$D_t = \max\{0, A_t - K + \max\{0, U_{t-1} - C_t\}\}, \tag{24}$$

which depends on $A_t$, $U_{t-1}$, and $C_t$. We are interested in finding the stationary behavior of $D_t$, as $t \to \infty$. Let us define $(U, C) := \lim\limits_{t \to \infty} (U_{t-1}, C_t)$, where the existence of a stationary distribution for the state pair $(U_{t-1}, C_t)$ was established in Section III-C. Since Poisson processes have independent increments [2], i.e., $A_t$ is independent of $t$, the limiting stationary distribution of $A_t$ exists as $t \to \infty$. Letting $A := \lim\limits_{t \to \infty} A_t$, we have:

$$P(A = a) = P(A_t = a), \tag{25}$$

and $E\{A\} = E\{A_t\} = \lambda T_f$. Based on (24), the stationary distribution of $D_t$ exists and is given by:

$$D := \lim_{t \to \infty} D_t = \max\{0, A - K + \max\{0, U - C\}\} \,. \tag{26}$$

Using (26), the ensemble-average number of packets dropped per time-unit can be calculated as:

$$\begin{aligned} E\{D\} = \sum_{a \in \mathcal{A}, u \in \mathcal{U}, c \in \mathcal{C}} &\max\{0, a - K + \max\{0, u - c\}\} \\ &\cdot P(A = a) \cdot P(U = u, C = c), \end{aligned} \tag{27}$$

where the equality follows because the arrival process is independent of the queue and the queue server states. Based on (25) and (27), we can compute $P_d$ as:

$$P_d := \lim_{T \to \infty} \frac{\sum_{t=1}^{T} D_t}{\sum_{t=1}^{T} A_t} = \frac{E\{D\}}{E\{A\}} = \frac{E\{D\}}{\lambda T_f} \,, \tag{28}$$

where the time average dropping probability equals its ensemble counterpart [5]. With $P_d$, $P_0$, and $\lambda T_f$ available, we can now compute $\xi$ and $\eta$ from (22) and (23), respectively.

## IV. Cross-Layer Design

Given certain parameters $f_d$, $\bar{\gamma}$, and $m$, it is desirable to optimize system performance metrics (such as $\xi$ and $\eta$), through optimizing $P_0$, $K$, $\lambda$, and $T_f$, subject to practical constraints. As a simple example, we here fix ($K$, $\lambda$, $T_f$), and only optimize $P_0$ in AMC to minimize $\xi$, which also maximizes $\eta$ as shown in (23).

Notice that $P_0$ affects $\xi$ in (22) in two different ways. It directly controls the packet error rate over wireless links at the physical layer, and also indirectly affects the packet dropping probability $P_d$ at the data link layer. Hence, a simple approach is to numerically find the optimal $P_0$ among all possible choices, as we detail next:

**Step 1**: Compute $\xi(P_0)$ from (22) for each $P_0 \in \mathcal{P}$, where $\mathcal{P}$ is the set of possible target PER values, e.g., $\mathcal{P} = \{P_0 : 0 < P_0 < 1\}$.

**Step 2**: Determine the optimal $P_0$ as:

$$P_0^{\text{opt}} = \arg\min_{P_0 \in \mathcal{P}} \xi(P_0) \, . \tag{29}$$

These steps are repeated, each time the system parameters $f_d$, $\bar{\gamma}$, $m$, $K$, $\lambda$, $T_f$ are updated.

Notice that $\xi(P_0)$ in Step 1 is affected by parameters at the data link layer, namely $K$ and $\lambda$, through $P_d$. Thus, the optimal $P_0^{\text{opt}}$ at the physical layer in Step 2 takes into account the data link layer characteristics. This simple example offers indeed a *cross-layer design* paradigm. As we will confirm by numerical results, such designs improve the system performance relative to the case where $P_0$ is set "blindly" at the physical layer without taking into account upper layers.

## V. Numerical Results

In this section, we present numerical results for TM. We assume that the frame length is $T_f = 2$ (ms) and $b = 2$. We fix the set of reference parameters as follows: average SNR $\bar{\gamma} = 15$ (dB); Doppler frequency $f_d = 10$ (Hz), i.e., $f_d T_f = 0.02$; Nakagami fading parameter $m = 1$; queue length $K = 50$ (packets), and Poisson arrival rate $\lambda T_f = 2$ (packets/time-unit).

We plot $\xi$ as a function of $P_0$ in Fig. 5. For each curve, we modify only one parameter from the reference parameters. We consider the following parameters:

1. Poisson arrival rate $\lambda T_f = 1.6$ (packets/time-unit);
2. Nakagami parameter $m = 1.1$;
3. queue length $K = 100$ (packets);
4. Doppler frequency $f_d = 5$ (Hz), i.e., $f_d T_f = 0.01$.

Comparing the curves in Fig. 5, we infer that:

1. Reducing the arrival data rate via decreasing $\lambda$ leads to small $P_d$, and thus lowers $\xi$;
2. Improving channel quality via increasing $m$ reduces packet reception errors; so, $\xi$ decreases;
3. Increasing queue length $K$ decreases $P_d$, which decreases $\xi$; and
4. A lower Doppler frequency $f_d$ leads to longer fading-duration, which increases $\xi$.

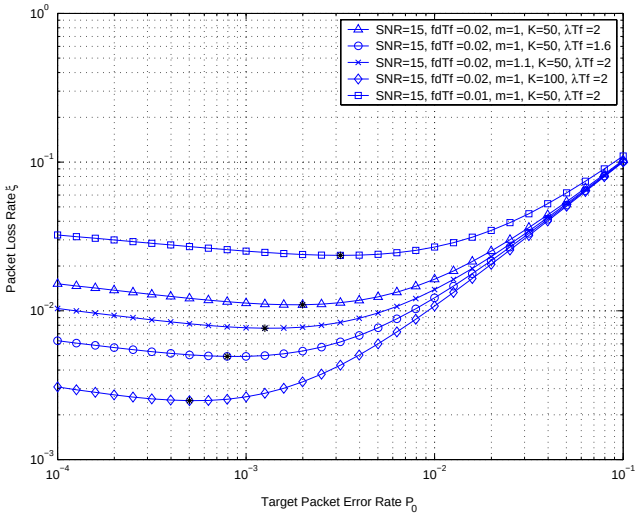


Fig. 5. Packet loss rate vs. target packet error rate

On each curve in Fig. 5, the minimum value of $\xi$ is depicted by star; the corresponding $P_0$ is the solution of our cross layer design in (29).

## Acknowledgment

The authors would like to thank Prof. W. L. Cooper, Univ. of Minnesota, for his suggestions on the queuing analysis and theorem proofs.

## References

[1] M. -S. Alouini and A. J. Goldsmith, "Adaptive modulation over Nakagami fading channels," *Kluwer Journal on Wireless Commun.*, vol. 13, no. 1–2, pp. 119–143, May 2000.

[2] D. Bertsekas and R. Gallager, *Data Networks*, Upper Saddle River, NJ: Prentice-Hall, 2nd Edition, 1992.

[3] A. Doufexi, S. Armour, M. Butler, A. Nix, D. Bull, J. McGeehan, and P. Karlsson, "A comparison of the HIPERLAN/2 and IEEE 802.11a wireless LAN standards," *IEEE Commun. Mag.*, vol. 40, no. 5, pp. 172–180, May 2002.

[4] Q. Liu, S. Zhou, and G. B. Giannakis, "Cross-Layer Combining of Adaptive Modulation and Coding with Truncated ARQ over Wireless Links," *IEEE Trans. Wireless Comm.*, 2004 (to appear).

[5] Q. Liu, S. Zhou, and G. B. Giannakis, "Queuing with Adaptive Modulation and Coding over Wireless Links: Cross-Layer Analysis and Design," *IEEE Trans. Wireless Comm.*, 2003 (submitted).

[6] H. K. Shiu, Y. H. Chang, T. C. Hou, and C. S. Wu, "Performance analysis of TCP over wireless link with dedicated buffers and link level error control," in *Proc. of Int. Conf. Commun.*, vol. 10, pp. 3211–3216, Amsterdam, Netherlands, June 30 – July 3, 2001.

[7] G. L. Stüber, *Principles of Mobile Communication*. Norwell, MA: Kluwer Academic, 2nd Edition, 2001.

[8] M. D. Yacoub, J. E. Vargas Bautista, and L. G. de R. Guedes, "On higher order statistics of the Nakagami-$m$ distribution," *IEEE Trans. Veh. Technol.*, vol. 48, no. 3, pp. 790–794, May 1999.

[9] Q. Zhang and S. A. Kassam, "Finite-state Markov model for Rayleigh fading channels," *IEEE Trans. Commun.*, vol. 47, no. 11, pp. 1688–1692, Nov. 1999.

[10] H. Zheng and J. Boyce, "An improved UDP protocol for video transmission over Internet-to-wireless networks," *IEEE Trans. Multimedia*, vol. 3, no. 3, pp. 356–365, Sept. 2001.